Isochoric *PVTx* Measurements for the CO_2 + N_2O System

Giovanni Di Nicola,* Giuliano Giuliani, and Fabio Polonara

Dipartimento di Energetica, Università Politecnica delle Marche, Via Brecce Bianche, 60100 Ancona, Italy

Roman Stryjek

Institute of Physical Chemistry, Polish Academy of Sciences, Warsaw, Poland

Measurements are reported for the CO_2 + N_2O system in both the two-phase and the superheated vapor regions using an isochoric apparatus. The experiment covered a temperature range from (214 to 358) K and a pressure range from (460 to 5870) kPa along 12 isochores. The data in the two-phase region enabled VLE to be estimated using a flash method with the Carnahan−Starling−De Santis equation of state (CSD EOS); in addition, the dew point for each isochore was found from the intersection of $P-T$ sequences. These dew-point values were also used to derive VLE. The data in the superheated region were compared with the predicted data with the virial equation of state, and agreement within an AAD = 1.2% was found.

Introduction

The number of chemicals that might be used in refrigeration for low-temperature applications is limited. Many of the chemicals that show a finite value of the ODP cannot be considered as a result of the Montreal protocol and its amendments. A further limitation results from the Kyoto protocol and, in Europe, from European directives imposing limitations on the emission of greenhouse gases responsible for global warming.

Nitrous oxide seems to be among the chemicals applicable in refrigeration at low temperatures. It is very similar to carbon dioxide in its critical parameters and saturated pressures. Its main advantage over carbon dioxide is its very low melting temperature. Its global warming potential (GWP = 310) is rather small but not negligible. Mixtures of carbon dioxide and nitrous oxide offer both low freezing temperatures and small GWP values.

Even if the carbon dioxide + nitrous oxide system is formed with components suitable for low-temperature application in refrigeration, thermophysical property information is limited. VLE was measured by Caubert[1] and by Cook.[2] The measurements of Cook cover a narrow temperature range close to the critical temperatures of the system constituents. There is a lack of VLE data at lower temperatures. To furnish the missing VLE data at low temperatures, isochoric measurements covering the temperature range from (214 to 358) K were made. From the data, the VLE parameters were derived via the Carnahan−Starling−De Santis equation of state.[3] The VLE data were shown over the whole temperature range of the system to be almost ideal in terms of Raoult's law, and because of small differences in saturated pressures of the system constituents, there are very small differences between the compositions of the liquid and vapor phases at equilibrium. This means that the system may be considered to be quasi-azeotropic over the full range of composition. No doubt, this is a very interesting case offering some advantages in mixture selection for low-temperature application because in practice a change in composition and a glide in the evaporation and condensation processes can be disregarded in total. Also, data on the solubility of carbon dioxide and nitrous oxide in *N*-dodecane[4] that show a significantly greater solubility of nitrous oxide might be considered to be promising in the possible use of natural lubricants, namely, paraffinic or naphthenic mineral oils.

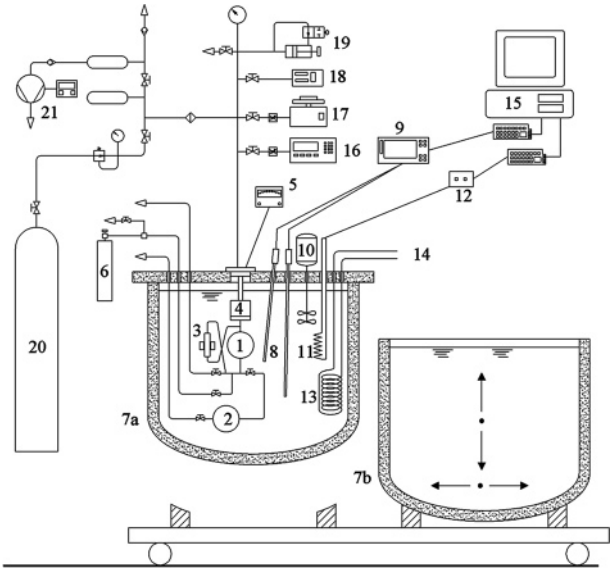

Figure 1. Schematic illustration of the apparatus.

Experimental Section

Chemicals. Carbon dioxide and nitrous oxide were supplied by Sol SpA. Their purity was checked by gas chromatography using a thermal conductivity detector and was found to be 99.99% for both fluids, basing all estimations on an area response.

Apparatus. The experimental setup is illustrated in Figure 1. The experimental setup was as described else-

* Corresponding author. E-mail: anfreddo@univpm.it.

10.1021/je049633+ CCC: $30.25
Published on Web 02/05/2005

Table 1. Investigated Compositions for the CO_2 (1) + N_2O (2) System

	T/K	P/kPa		m/g[b]		dew point	
z_1[a]	range	range	N/mol	(1)	(2)	T/K	P/kPa
0.0902	217−348	512−4593	0.53346	2.118	21.359	272	3076
0.1499	214−358	460−3293	0.33929	2.239	12.693	257	2072
0.2607	215−358	482−3470	0.36011	4.132	11.716	259	2187
0.3585	216−358	511−4402	0.47168	8.065	12.693	267	2797
0.4754	217−358	532−3823	0.40882	8.553	9.439	261	2413
0.5959	217−358	534−1630	0.16009	4.198	2.847	233	981
0.6099	215−343	491−5579	0.68239	18.316	11.716	278	3788
0.6929	217−358	538−5227	0.56301	17.168	7.611	272	3319
0.6953	218−358	550−2136	0.21228	6.496	2.847	241	1301
0.7478	217−358	535−4567	0.48871	16.084	5.424	267	2885
0.8378	223−333	685−5868	0.75967	28.009	5.424	281	4185
0.9071	216−358	514−4192	0.43006	17.168	1.759	263	2635

[a] z_1 denotes the charged bulk composition. [b] m denotes the mass charge.

where,[5] so it is only briefly outlined here. The main modification to the original apparatus[6,7] concerned the twin thermostatic baths (7) filled with different silicone oils (Baysilone M10 and Baysilone M100, Bayer). After being charged with the sample mixture, the apparatus can be operated over two temperature ranges, roughly from (210 to 290) K and from (290 to 360) K, depending on which bath is used. The thermostatic baths were easy to move because of the new configuration of the system. The spherical cells and pressure transducer were immersed in one of the two thermostatic baths (7). An auxiliary thermostat (14) was used to reach below-ambient temperatures. The cell volume, estimated as reported elsewhere,[5] was found to be (273.5 ± 0.3) cm^3 at room temperature.

The pressure and temperature data acquisition systems remained the same as for the previous apparatus.[6,7] Temperature was controlled by a PID device and measured with a calibrated resistance thermometer; the temperature's total uncertainty was found to be lower than ±0.02 K. The uncertainty in the pressure measurements was due to the uncertainty of the transducer and null indicator system and the pressure gauges. The digital pressure indicator (Ruska, model 7000) had an uncertainty of ±0.003% of its full scale. The total uncertainty in the pressure measurement was also influenced by temperature fluctuations due to bath instability; it was found to be less than ±1 kPa.

Experimental Procedure. Mixtures were prepared using the gravimetric method. The pure samples were first placed into different bottles, degassed to remove noncondensable gases and air, and weighed with an analytical balance (uncertainty ±0.3 mg). After evacuating the cell, we then discharged the bottles into the cell immersed in the bath. At the end of this procedure, the bottles were weighed, and the mass of the charge was calculated from the difference between the two weights. The dispersion of the mass inside the duct was estimated to be between 0.01 and 0.06 g, depending on the charging temperature, pressure, and molar mass of the single fluid, and finally subtracted from the total mass of the charge. The uncertainty in composition measurements was estimated to be always lower than 0.1% in mole fraction.

During the experiment, after reaching the desired temperature, the magnetic pump was operated for about half an hour; next, after about half an hour, the temperature and pressures were recorded.

Results and Discussion

The temperature and pressure ranges are shown in Table 1, along with the mixture's composition and the number of moles charged.

Table 2. Experimental Data within the VLE Boundary for the CO_2 (1) + N_2O (2) System

	T	P	V		T	P	V		T	P	V		T	P	V
z_1	K	kPa	dm^3/mol	z_1	K	kPa	dm^3/mol	z_1	K	kPa	dm^3/mol	z_1	K	kPa	dm^3/mol
0.0902				0.3585				0.6099				0.7478			
	217.13	516.2	0.511		216.32	511.3	0.578		243.12	1409.0	0.400		248.10	1668.0	0.559
	223.11	656.7	0.511		223.11	675.5	0.578		248.10	1655.0	0.400		253.09	1950.1	0.559
	228.06	792.5	0.511		228.13	819.5	0.579		253.10	1931.6	0.400		258.07	2261.7	0.559
	233.04	949.3	0.512		233.12	983.3	0.579		258.10	2241.4	0.400		263.04	2608.8	0.559
	238.03	1127.6	0.512		238.11	1170.7	0.579		263.08	2583.3	0.400	0.8378			
	243.06	1335.3	0.512		243.10	1383.6	0.579		268.08	2964.2	0.401		223.12	684.6	0.359
	248.03	1563.1	0.512		248.09	1623.1	0.579		273.06	3382.5	0.401		228.10	832.0	0.359
	253.01	1819.3	0.512		253.07	1891.3	0.579	0.6929					233.08	1002.8	0.359
	258.09	2112.6	0.512		258.08	2192.9	0.579		217.13	538.4	0.484		238.09	1196.9	0.359
	263.07	2427.9	0.512		263.10	2527.5	0.579		220.10	609.5	0.484		243.06	1421.1	0.359
	268.12	2783.9	0.512	0.4754					223.08	687.6	0.484		248.07	1674.3	0.359
0.1499					217.13	531.7	0.667		228.11	834.9	0.485		253.05	1956.0	0.360
	214.24	459.5	0.804		223.11	678.5	0.667		232.99	1001.0	0.485		258.04	2271.7	0.360
	218.14	541.3	0.804		228.21	826.1	0.667		238.04	1195.8	0.485		263.10	2629.5	0.360
	223.11	661.3	0.804		233.10	988.8	0.667		243.03	1415.1	0.485		268.07	3018.0	0.360
	228.14	801.1	0.804		238.09	1177.9	0.668		248.07	1667.4	0.485		272.97	3442.4	0.360
	233.13	959.5	0.804		243.07	1391.5	0.668		253.01	1943.9	0.485		277.84	3905.7	0.360
	238.11	1141.0	0.804		248.10	1636.1	0.668		258.00	2252.3	0.485	0.9071			
	243.13	1347.7	0.805		253.03	1904.1	0.668		262.98	2596.9	0.485		216.13	514.3	0.634
	248.12	1579.1	0.805		258.09	2209.8	0.668		267.95	2982.5	0.485		218.12	560.0	0.634
	253.11	1838.5	0.805	0.5959				0.6953					223.08	687.4	0.634
0.2607					217.14	534.0	1.703		217.79	550.2	1.285		228.10	836.5	0.634
	215.13	482.2	0.757		223.11	682.1	1.704		223.11	684.7	1.285		233.04	1006.2	0.635
	218.13	546.8	0.757		228.12	828.9	1.704		228.12	831.9	1.285		238.07	1203.8	0.635
	223.12	668.6	0.757		233.09	975.1	1.705		233.12	1001.5	1.285		243.05	1427.1	0.635
	228.14	810.5	0.758	0.6099				0.7478					248.07	1681.4	0.635
	233.13	971.5	0.758		215.14	490.6	0.400		217.14	534.9	0.558		253.05	1964.8	0.635
	238.11	1156.0	0.758		218.12	557.4	0.400		223.11	684.9	0.558		258.03	2281.9	0.635
	243.10	1365.0	0.758		223.08	682.8	0.400		228.08	831.5	0.558				
	248.11	1601.3	0.758		228.13	830.0	0.400		233.05	1000.0	0.558				
	253.10	1864.6	0.758		233.07	996.6	0.400		238.08	1195.4	0.558				
	258.10	2153.3	0.759		238.12	1190.6	0.400		243.07	1417.4	0.559				

Table 3. Experimental Data in the Superheated Vapor Region for the CO_2 (1) + N_2O (2) System

	T	*P*	*V*		*T*	*P*	*V*		*T*	*P*	*V*		*T*	*P*	*V*
z_1	K	kPa	dm³/mol	z_1	K	kPa	dm³/mol	z_1	K	kPa	dm³/mol	z_1	K	kPa	dm³/mol
0.0902				0.3585				0.6099				0.7478			
	272.98	3090.5	0.512		292.98	3279.6	0.580		277.86	3791.0	0.401		268.08	2907.1	0.559
	277.82	3196.6	0.513		303.02	3458.7	0.580		282.82	3939.5	0.401		273.06	3007.9	0.559
	282.66	3300.1	0.513		307.97	3546.3	0.580		292.89	4229.6	0.401		277.87	3104.0	0.559
	292.79	3511.2	0.513		318.04	3722.1	0.581		297.92	4370.8	0.401		283.01	3203.9	0.560
	298.05	3617.5	0.513		327.94	3893.1	0.581		307.87	4646.1	0.401		292.99	3397.0	0.560
	308.02	3818.3	0.513		338.08	4065.8	0.581		317.84	4915.4	0.401		298.06	3490.8	0.560
	318.05	4013.5	0.513		348.07	4234.7	0.582		323.12	5055.4	0.401		308.03	3676.1	0.560
	328.11	4212.5	0.514		358.04	4401.6	0.582		328.11	5188.2	0.402		318.13	3860.5	0.560
	338.03	4402.1	0.514	0.4754					338.09	5449.4	0.402		328.10	4040.6	0.561
	348.02	4592.8	0.514		263.10	2436.3	0.668		343.08	5578.9	0.402		338.07	4218.4	0.561
0.1499					268.08	2515.8	0.669	0.6929					348.06	4394.9	0.561
	258.09	2081.3	0.805		273.07	2593.6	0.669		272.93	3330.4	0.486		357.91	4567.0	0.561
	263.06	2148.3	0.805		282.82	2743.7	0.669		277.94	3453.5	0.486	0.8378			
	268.03	2212.6	0.806		293.06	2897.6	0.669		283.01	3574.6	0.486		282.83	4250.2	0.360
	273.12	2276.8	0.806		298.04	2970.8	0.669		293.06	3809.7	0.486		292.99	4597.0	0.360
	283.01	2401.3	0.806		308.13	3117.6	0.670		298.04	3923.4	0.486		299.02	4795.1	0.360
	292.97	2524.4	0.806		318.11	3261.7	0.670		308.00	4148.1	0.486		308.09	5087.6	0.360
	302.04	2647.7	0.807		328.09	3404.0	0.670		318.12	4371.8	0.486		318.02	5401.8	0.361
	312.22	2766.9	0.807		338.11	3545.6	0.671		328.10	4589.4	0.487		322.91	5554.6	0.361
	323.11	2885.7	0.807		348.05	3684.7	0.671		338.07	4804.3	0.487		328.00	5712.0	0.361
	333.09	3003.3	0.808		358.02	3823.2	0.671		348.06	5017.1	0.487		333.10	5868.1	0.361
	343.08	3119.8	0.808	0.5959					357.99	5226.8	0.487	0.9071			
	353.04	3235.1	0.809		238.10	1004.5	1.705	0.6953					263.02	2626.7	0.638
	358.04	3292.6	0.809		243.07	1032.4	1.705		238.10	1194.6	1.286		268.02	2719.9	0.635
0.2607					248.05	1059.7	1.706		243.09	1317.0	1.286		273.04	2808.9	0.636
	263.09	2245.7	0.759		253.04	1086.8	1.706		248.11	1355.8	1.286		282.90	2980.0	0.636
	273.05	2384.1	0.759		263.08	1140.7	1.707		253.10	1393.5	1.287		293.06	3153.2	0.636
	283.01	2518.2	0.759		268.04	1168.2	1.707		258.11	1431.2	1.287		298.04	3235.8	0.636
	293.11	2651.8	0.760		272.93	1194.4	1.708		263.08	1469.0	1.287		308.01	3399.4	0.637
	303.13	2781.5	0.760		282.83	1245.4	1.708		263.05	1469.0	1.287		318.12	3563.0	0.637
	308.07	2845.0	0.760		292.98	1297.8	1.709	0.6953					328.10	3722.5	0.637
	318.01	2971.6	0.761		298.04	1323.7	1.709		268.05	1505.5	1.287		338.08	3880.7	0.637
	327.98	3097.5	0.761		308.00	1375.9	1.710		272.94	1541.4	1.288		348.06	4036.9	0.638
	338.09	3223.8	0.761	0.5959					282.33	1612.9	1.288		358.03	4191.9	0.638
	348.05	3346.9	0.762		318.11	1427.6	1.711		292.97	1685.2	1.289				
	358.02	3469.7	0.762		328.09	1478.4	1.712		308.00	1790.6	1.290				
0.3585					338.07	1529.0	1.712		318.12	1861.3	1.290				
	268.08	2813.7	0.579		348.06	1579.5	1.713		328.10	1930.7	1.291				
	272.95	2909.1	0.580		357.99	1629.5	1.714		338.08	1999.6	1.291				
	282.84	3094.9	0.580						348.06	2068.1	1.292				
									357.95	2135.6	1.293				

Analyzing the slope of each *T*−*P* sequence, we attributed each experimental point either to the superheated or to the two-phase region. The experimental data within the VLE boundary are given in Table 2, whereas Table 3 shows the *PVTx* data. The number of data belonging to each region is also included in Table 1. The data belonging to the two-phase region were fitted by the Antoine equation, whereas the data in the superheated region were fitted by a second-degree polynomial, taking temperature as the independent variable. Then, from the solution of the two equations representing the system's behavior in the two-phase and superheated regions, the temperature and pressure corresponding to the dew point were found algebraically for each isochore. The solutions are given in Table 1.

VLE Derivation. Two methods were used to derive VLE data from the isochoric measurements, as described elsewhere.[8]

In the first, the VLE parameters were derived using the dew-point method with the CSD EOS. The uncertainties in the temperature and pressure of the dew points arising from the error distribution of the data correlated with the Antoine and polynomial equations were estimated to be on the order of ±0.3 K and ±1 kPa, respectively. The necessary dew-point parameters (Table 1) were used as independent variables, whereas the interaction binary parameter k_{12} and the corresponding pressure and liquid-phase composition at the bubble point (considered as dependent variables) were adjusted until the phase equilibrium condition was reached. The resulting k_{12} values and bubble-point parameters are shown in Table 4.

Table 4. Binary Interaction Parameters and Bubble-Point Composition (x_1) for CO_2 (1) + N_2O (2) Found from the Dew Point by Applying the CSD EOS

	CO_2 (1) + N_2O (2)		
	k_{12dew}	$k_{12flash}$	x_1
	−0.0296	−0.0363	0.0967
	−0.0201	−0.0183	0.1562
	−0.0095	−0.0075	0.2582
	−0.0011	−0.0024	0.3479
	−0.0013	−0.0008	0.4644
	−0.0070	−0.0003	0.5888
	0.0026	0.0016	0.5980
	0.0039	0.0040	0.6837
	0.0022	0.0031	0.6910
	0.0030	0.0027	0.7403
	0.0064	0.0035	0.8333
	0.0062	0.0092	0.9059
av	−0.0037	−0.0037	

In the second method, the VLE parameters were derived for each data point in the two-phase region using the flash method with the CSD EOS. To apply the flash method to isochoric data, the volumetric properties of both phases are also needed and were calculated from the CSD EOS. During the fitting procedure, *T*, *P*, *zi*, and *n* (number of moles charged) were kept constant for each experimental

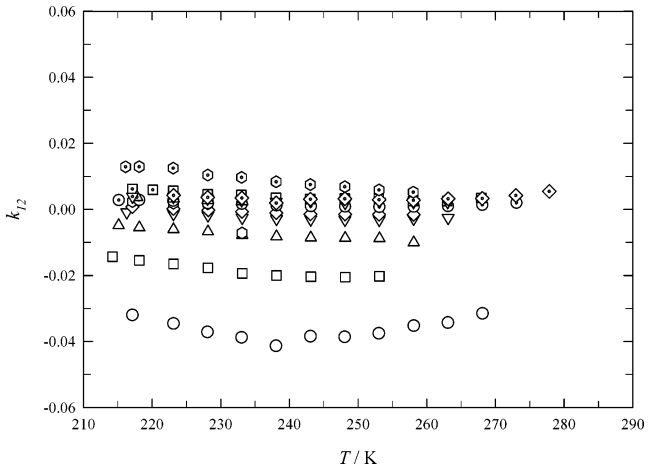

Figure 2. k_{12} values found by the flash method for the CO_2 (1) + N_2O (2) system.

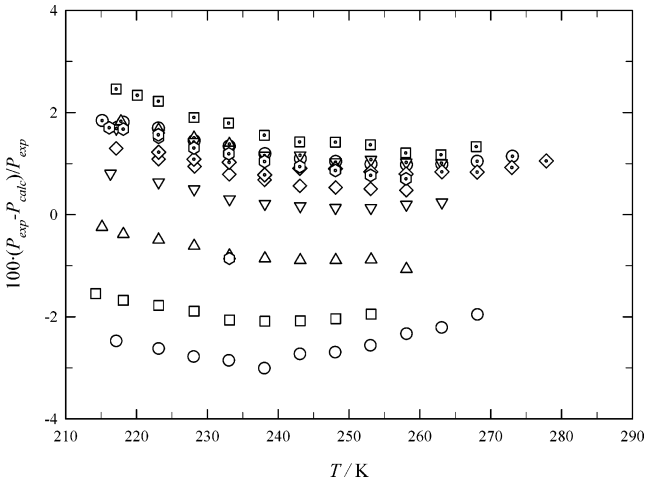

Figure 3. Deviations in pressure between experimental values and those calculated with the k_{12} coefficients for the CO_2 (1) + N_2O (2) system. Signs are as denoted in Figure 2.

point. Because the isochoric cell volume was known from the gravimetric calibration, the binary interaction parameter k_{12} and the composition at the bubble and dew points were found, considering them to be dependent variables. The k_{12} values found for each data point in the two-phase region are shown in Figure 2, whereas the scatter diagram of the relative deviations in pressure is reported in Figure 3. The binary interaction parameters showed almost temperature-independent behavior, and the deviations in pressure were found to be around ±2%.

Using averaged values of k_{12} from our measurements in the two-phase region, the VLE was calculated at three temperatures. The results are shown in Figure 4. Each line represents pressures along the bubble and dew points, being graphically indistinguishable because of small differences in the courses of two branches of the VLE boundary.

The excess Gibbs energy is calculated from eq 1

$$G^{\mathrm{E}} = RT(\ln \phi - \sum x_i \phi_i) \tag{1}$$

where ϕ and ϕ_i stand for the fugacity coefficients of the mixtures and pure components, respectively, at the same temperature T and pressure P and R is the gas constant showing only a small temperature dependence. The course of the G^{E} at T = 243.15 K is shown in Figure 5.

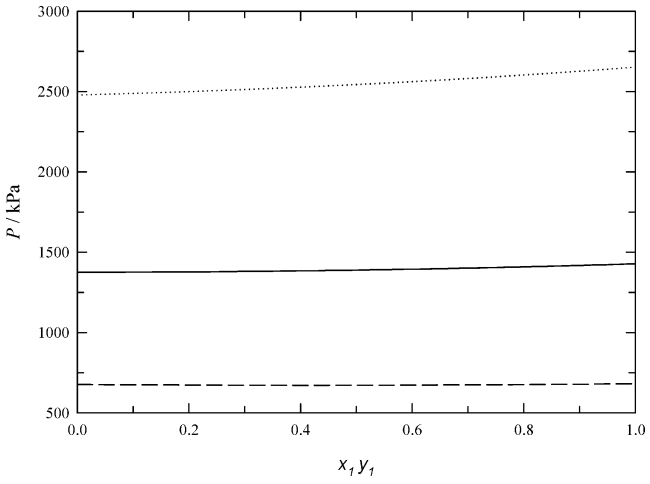

Figure 4. VLE calculated from the CSD EOS for the CO_2 (1) + N_2O (2) system at three temperatures: T = 223.15 K (- - -), T = 243.15 K (−), and T = 263.15 K (···). Each line represents both the bubble and dew points.

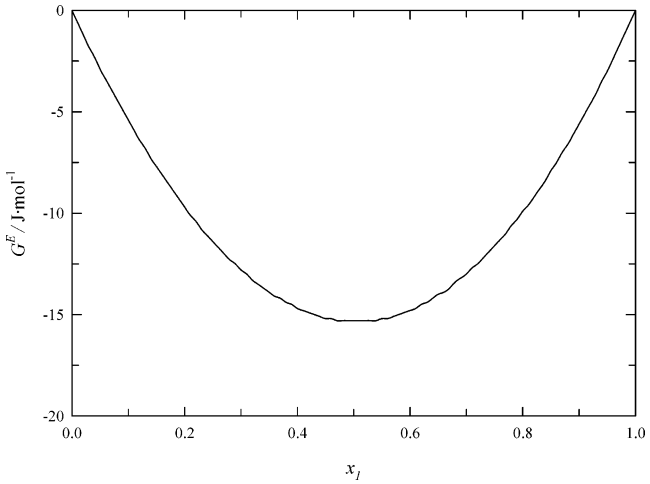

Figure 5. Excess Gibbs energy for the CO_2 (1) + N_2O (2) system at T = 243.15 K.

PVTx. Because of the complete lack of published data on the superheated vapor region for the binary systems considered, our experimental *PVTx* findings were compared with data calculated with the virial EOS in the Leiden form. A simple polynomial temperature dependence was found for the second and the third virial coefficients. Then, the pressure values were calculated from the virial equation of state adopting the isochoric experimental temperatures and molar volumes. The second and third virial coefficients for the two pure fluids (B_{ii}, B_{jj}, C_{iii}, and C_{jjj}) were taken from our previous Burnett experiments,[9,10] whereas for the cross virial coefficients (B_{ij}, C_{iij}, and C_{ijj}), because the binary system showed almost ideal behavior, the following "naïve" expressions were adopted:

$$B_{ij} = \frac{B_{ii} + B_{jj}}{2} \tag{2}$$

$$C_{iij} = \frac{2C_{iii} + C_{jjj}}{3} \tag{3}$$

$$C_{ijj} = \frac{C_{iii} + 2C_{jjj}}{3} \tag{4}$$

The results are shown in Figure 6, where the relative deviations in pressure are shown. Considering that the

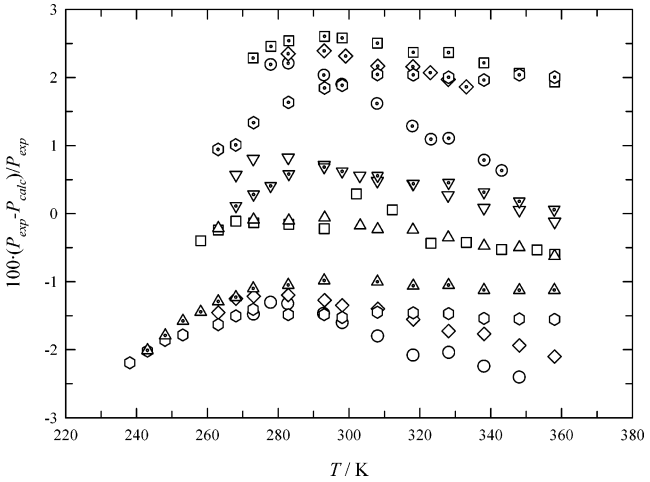

Figure 6. Relative pressure deviations for the CO_2 (1) + N_2O (2) system between experimental values from isochoric data and data calculated with the virial EOS. Signs are as denoted in Figure 2.

comparison is based on estimations through equations containing from two to four cross virial coefficients and that the temperature dependence of the virial coefficients was represented with simple third-degree polynomial expressions, the deviations are clearly randomly distributed along the temperature, and we found that AAD = 1.2% can be considered satisfactory.

Conclusions

A new isochoric apparatus was used for *PVTx* measurements on the CO_2 + N_2O system. The binary interaction parameters were derived from experimental data in the two-phase region, applying the flash method and the Carnahan−Starling−DeSantis equation of state (CSD EOS). The dew-point parameters were found by interpolating the $P-T$ isochoric sequences, again applying the CSD EOS. The calculated binary interaction parameters were used to derive the VLE parameters. The derived VLE data showed that the system is almost ideal in term of Raoult's law with the G^E value at $x_1 = 0.5$ and $T = 233.15$ K below −20 J/mol. The *PVTx* data are consistent with the values predicted by the virial equation of state using its coefficients for the system constituents derived from independent measurements.

Acknowledgment

This work was supported by MIUR, Ministry of Instruction, University and Research, and by the government of the Marche region.

Literature Cited

(1) Caubert, F. The condensation of gas mixtures. *Z. Phys. Chem.* **1904**, *49*, 101−116.
(2) Cook, D. The carbon dioxide-nitrous oxide system in the critical region. *Proc. R. Soc. London, Ser. A* **1953**, *219*, 245−256.
(3) De Santis, R.; Gironi, F.; Marrelli, L. Vapor-Liquid Equilibrium from a Hard-Sphere Equation of State. *Ind. Eng. Chem. Fundam.* **1976**, *15*, 183−189.
(4) Henni, A.; Jaffer, S.; Mather, A. E. Solubility of N_2O and CO_2 in n-Dodecane. *Can. J. Chem. Eng.* **1996**, *74*, 554−557.
(5) Di Nicola, G.; Polonara, F.; Ricci, R.; Stryjek, R. *PVTx* Measurements for the R116 + CO_2 and R41 + CO_2 Systems. New Isochoric Apparatus. *J. Chem. Eng. Data*, in press, 2005
(6) Giuliani, G.; Kumar, S.; Zazzini, P.; Polonara, F. Vapor Pressure and Gas-Phase PVT Data and Correlation for 1,1,1,-Trifluoroethane (R143a). *J. Chem. Eng. Data* **1995**, *40*, 903−908.
(7) Giuliani, G.; Kumar, S.; Polonara, F. A Constant Volume Apparatus for Vapour Pressure and Gas Phase *P-v-T* Measurements: Validation with Data for R22 and R134a. *Fluid Phase Equilib.* **1995**, *109*, 265−279.
(8) Di Nicola, G.; Giuliani, G.; Passerini, G.; Polonara, F.; Stryjek, R. Vapor-Liquid Equilibria (VLE) Properties of R-32 + R-134a System Derived from Isochoric Measurements. *Fluid Phase Equilib.* **1998**, *153*, 143−165.
(9) Di Nicola, G.; Giuliani, G.; Polonara, F.; Stryjek, R. *PVTx* Measurements for the R125+CO_2 System by the Burnett Methodol. *Fluid Phase Equilib.* **2002**, *199*, 161−174.
(10) Di Nicola, G.; Giuliani, G.; Ricci R.; Stryjek, R. *PVT* Properties of Dinitrogen Monoxide. *J. Chem. Eng. Data* **2004**, *49*, 1465−1468.

Received for review October 18, 2004. Accepted December 28, 2004.

JE049633+